Available online at www.sciencedirect.com
SCIENCE DIRECT®
Journal of Power Sources 146 (2005) 259–263
JOURNAL OF POWER SOURCES
www.elsevier.com/locate/jpowsour

Redox behaviour of iron during delithiation in $Li_xCo_{1-y}Fe_yO_2$ solid solution: An in situ ^{57}Fe Mössbauer study

Laurent Aldon [a], Josette Olivier-Fourcade [a], Jean-Claude Jumas [a,*], Michael Holzapfel [b,1], Céline Darie [c], Pierre Strobel [c]

[a] *Laboratoire des Agrégats Moléculaires et Matériaux Inorganiques (UMR 5072 CNRS), Université Montpellier II, CC15, Place Eugène Bataillon, F-34095 Montpellier Cedex 5, France*
[b] *Laboratoire des Champs Magnétiques Intenses, MPI-FKF, BP 166, F-38042 Grenoble Cedex 9, France*
[c] *Laboratoire de Cristallographie (UPR 5031 CNRS), BP 166, F-38042 Grenoble Cedex 9, France*

Available online 31 May 2005

Abstract

The electronic changes occurring upon electrochemical delithiation of the $LiCo_{1-y}Fe_yO_2$ solid solution were characterised by means of in situ electrochemical ^{57}Fe Mössbauer spectroscopy on plastic batteries for $y = 0.1$, 0.2 and 0.4. For the $y = 0.1$ and 0.2 pristine materials, two quadrupole doublets were observed in the Mössbauer spectra. The first one, with an isomer shift of 0.32–0.33 mm s^{-1}, is ascribable to Fe^{III} replacing Co^{III} in the octahedral sites of the CoO_2 layer while the weaker second doublet, with an isomer shift of 0.24–0.19 mm s^{-1}, shows the presence of Fe^{III} in pseudotetrahedral sites of the Li_2O layers. For $y = 0.4$, all Fe^{III} atoms are located on the octahedral sites of the CoO_2 layer and the presence of α-$LiFeO_2$ as impurity was detected (16%). During the delithiation process the $Fe^{III} \rightarrow Fe^{IV}$ oxidation was clearly evidenced by the appearance of a new subspectrum with an isomer shift in the range −0.17 to −0.01 mm s^{-1} whose intensity increases with the amount of deintercalated lithium. In all cases the amount of oxidised iron Fe^{IV} does not exceed 56% of the total iron content, i.e. the oxidation of the Fe^{III} does not continue to completeness. This means that the oxidation of Fe^{III} and Co^{III} occurs simultaneously. The presence of iron in the Li_2O layer and the difficulty of complete oxidation of Fe^{III} can explain the poor reversibility of this process.

Keywords: Lithium iron oxide; Lithium cobalt oxide; Lithium-ion batteries; Lithium deintercalation; ^{57}Fe Mössbauer data

1. Introduction

Lithium cobalt oxide $LiCoO_2$ is at present the most widely used positive electrode material in commercial Li-ion batteries, due to its high reversible capacity (130–150 mAh g^{-1}) and life cycle (300–500 cycles) and its easy preparation. However, the search for increased reversible capacity, safety problems which related to the instability of the delithiated phase and environmental reasons have stimulated intensive research to replace Co [1,2]. An interesting alternative would be the partial substitution of Co by Fe in the $LiCo_{1-y}Fe_yO_2$ solid solution, because of the low cost and environmental friendliness of iron. Holzapfel et al. recently achieved an entire range of solid solution in this system using an ion exchange reaction $NaCo_{1-y}Fe_yO_2 \rightarrow LiCo_{1-y}Fe_yO_2$ [3]. Although many characterisations have been carried out on this system during lithium deintercalation [4–8], using ex situ X-ray diffraction, Co and Fe K-edge X-ray absorption and ^{57}Fe Mössbauer spectroscopies for the $LiCo_{0.8}Fe_{0.2}O_2$ composition [9], the role of iron in this system is not well understood. In order to determine the lithium deintercalation mechanism we have studied three compositions of the $LiCo_{1-y}Fe_yO_2$ solid solution ($y = 0.1$, 0.2 and 0.4) with in situ ^{57}Fe Mössbauer measurements upon electrochemical deintercalation. This hyperfine nuclear spectroscopy is of high interest for the study of mechanisms

* Corresponding author.
E-mail address: jumas@univ-montp2.fr (J.-C. Jumas).
[1] Present adress: Paul Scherrer Institut, CH-5232 Villigen PSI, France.

0378-7753/$ – see front matter © 2005 Elsevier B.V. All rights reserved.
doi:10.1016/j.jpowsour.2005.03.123

induced by lithium intercalation–deintercalation processes [10]. The hyperfine parameters isomer shift (IS) and quadrupole splitting (QS) are related to the oxidation states and local environments of the Fe probed element, respectively, and the proportions of different species can be determined from their relative contribution to the total spectral absorption.

2. Experimental

The preparation of the samples and the plastic batteries has been carried out as described in detail previously [6,11]. The charges of the plastic batteries were done with intermittent steps at C/5 rate (Fig. 1).

The Mössbauer data collection was performed during the subsequent rest time of the batteries at constant Li composition and at room temperature with a classical EG & G constant accelerator spectrometer using a ^{57}Co in a Rh matrix as γ-ray source. The velocity scale was calibrated using the magnetic sextuplet spectrum of a high purity iron foil absorber and the origin of the isomer shift scale was determined from the centre of the α-Fe spectrum. Experimental data were fitted to Lorentzian profiles by a least square method [12] and the fit quality was controlled by the classical χ^2 test.

3. Results and discussion

Table 1 summarises the ^{57}Fe Mössbauer hyperfine parameters calculated from the spectra of the $Li_{1-x}Co_{1-y}Fe_yO_2$ samples for $x = 0$ (pristine materials) and at different stages during the delithiation process ($x = 0.15$, 0.30, 0.45, 0.60, 0.75, 0.90).

Fig. 2 shows the Mössbauer spectra of the pristine samples with $LiCo_{1-y}Fe_yO_2$ stoichiometry. For $y = 0.1$ and 0.2 the principal quadrupole split sub-spectrum with an isomer shift of ca 0.32 mm s^{-1} is ascribable to Fe^{III} replacing Co^{III} in the CoO_2 layers. The second weak quadrupole doublet with an isomer shift in the range 0.19–0.24 mm s^{-1} and a quadrupole splitting of 0.42–0.57 mm s^{-1} could be assigned to Fe^{III} on pseudotetrahedral sites of the Li_2O layers. The contribution of this second doublet decreases as a function of the increasing iron content, and for $y = 0.4$ it entirely disappears. In this case another sub-spectrum with an isomer shift of 0.54 mm s^{-1} and weak quadrupole splitting of 0.05 mm s^{-1} is observed. Checking that there is no contribution of iron component from the cell and taking into account that this sub-spectrum is present during the full discharge, it has been ascribed to a Li–Fe oxide as impurity. This impurity has not been detected by X-ray diffraction in Refs. [3,6] because its percentage and crystallinity are too low. Among the Li–Fe oxides, $LiFeO_2$, not electrochemically active [5,13], presents several forms: α,

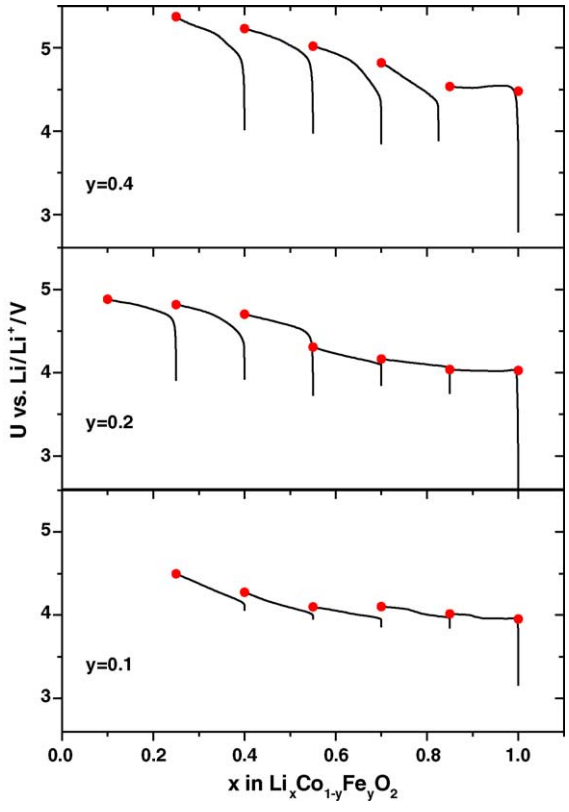

Fig. 1. Galvanostatic charge curves for $LiCo_{1-y}Fe_yO_2$ ($y = 0.1$, 0.2 and 0.4). Solid circles indicate the compositions at which ^{57}Fe Mössbauer spectra were recorded.

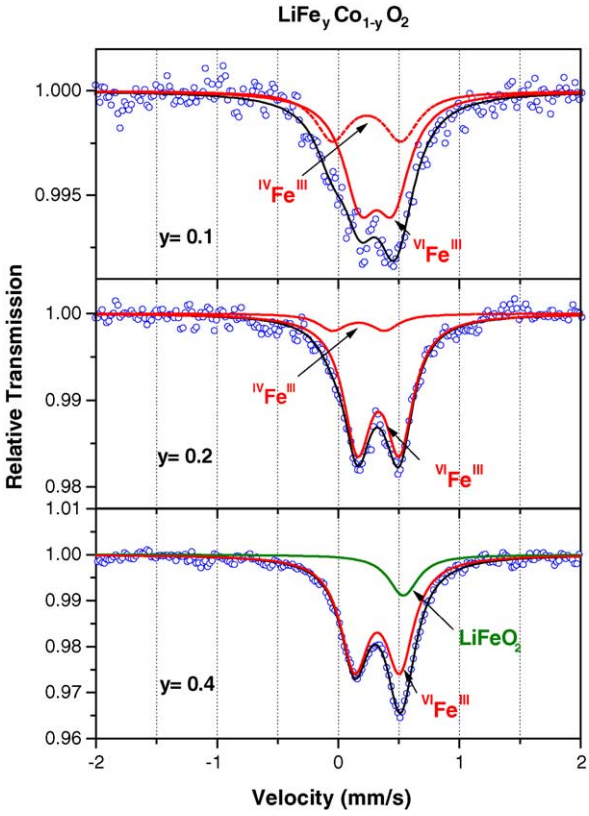

Fig. 2. ^{57}Fe Mössbauer spectra of the $LiCo_{1-y}Fe_yO_2$ pristine materials ($y = 0.1$, 0.2 and 0.4).

Table 1
^{57}Fe Mössbauer hyperfine parameters of $Li_{1-x}Co_{1-y}Fe_yO_2$ derived from the refined spectra shown in Figs. 2–5

x	$y = 0.1$				$y = 0.2$				$y = 0.4$			
	δ (mm s^{-1})	Δ (mm s^{-1})	Γ (mm s^{-1})	C (%)	δ (mm s^{-1})	Δ (mm s^{-1})	Γ (mm s^{-1})	C (%)	δ (mm s^{-1})	Δ (mm s^{-1})	Γ (mm s^{-1})	C (%)
0	0.32 (2)	0.27 (3)	0.34 (6)	68	0·33 (1)	0.34 (1)	0.27 (4)	86	0.32 (1)	0.37 (1)	0.28 (1)	84
	0.24 (4)	0.57 (6)	0.34 (6)	32	0.19 (3)	0.42 (3)	0.27 (4)	14	0.54 (4)	0.05 (6)	0.23 (1)	16
0.15	0.27 (3)	0.31 (1)	0.35 (5)	66	0.32 (1)	0.34 (1)	0.33 (4)	85	0.31 (1)	0.35 (1)	0.32 (2)	70
	0.18 (5)	0.41 (6)	0.35 (5)	19	–	–	–	–	0.54[a]	0.05[a]	0.32 (2)	16
	−0.17 (5)	0.37 (6)	0.35 (5)	15	−0.17 (4)	0.27 (4)	0.33 (4)	15	−0.13 (4)	0.24 (1)	0.32 (2)	14
0.30	0.27 (1)	0.26 (1)	0.35 (5)	71	0.26 (1)	0.39 (1)	0.37 (3)	69	0.27 (2)	0.37 (2)	0.42 (3)	56
	–	–	–	–	–	–	–	–	0.54[a]	0.05[a]	0.42 (3)	14
	−0.12 (4)	0.24 (4)	0.35 (5)	29	−0.02 (2)	0.38 (3)	0.37 (3)	31	−0.13 (4)	0.31 (4)	0.42 (3)	30
0.45	0.27 (3)	0.20 (3)	0.35 (4)	57	0.26 (1)	0.36 (1)	0.40 (1)	58	0.25 (3)	0.37 (3)	0.41 (3)	37
	–	–	–	–	–	–	–	–	0.54[a]	0.05[a]	0.41 (3)	15
	−0.05 (5)	0.22 (4)	0.35 (4)	43	−0.09 (2)	0.32 (2)	0.40 (1)	42	−0.08 (3)	0.34 (3)	0.41 (3)	48
0.60	0.33 (2)	0.18 (3)	0.37 (3)	45	0.28 (1)	0.35 (1)	0.41 (2)	48	0.20 (3)	0.35 (3)		
	0.39 (3)	36										
	–	–	–	–	–	–	–	–	0.54[a]	0.05[a]	0.41 (3)	15
	−0.05 (1)	0.21 (2)	0.37 (3)	55	−0.08 (1)	0.28 (1)	0.41 (2)	52	−0.11 (3)	0.34 (3)	0.39 (3)	49
0.75	0.32 (2)	0.25 (3)	0.42 (4)	46	0.29 (1)	0.34 (1)	0.43 (2)	45	0.20 (3)	0.28 (3)	0.40 (3)	35
	–	–	–	–	–	–	–	–	0.54[a]	0.05[a]	0.40 (3)	14
	−0.01 (3)	0.15 (6)	0.42 (4)	54	−0.12 (1)	0.28 (1)	0.43 (2)	55	−0.15 (3)	0.32 (3)	0.40 (3)	51
0.90					0.33 (1)	0.27 (1)	0.35 (2)	44				
					–	–	–	–				
					−0.13 (2)	0.25 (2)	0.35 (2)	56				

[a] Fixed parameter.

γ and β which are characterized by isomer shift in the range 0.37–0.55 mm s^{-1} [14–16]. In particular the β form, whose crystal structure would be tetragonal and disordered as cubic α-$LiFeO_2$ presents an isomer shift of 0.55 mm s^{-1} [15]. So this impurity could be attributed to a metastable amorphous form of $LiFeO_2$.

Figs. 3–5 show the Mössbauer spectra recorded during lithium deintercalation. For all samples, $Fe^{III} \rightarrow Fe^{IV}$ oxidation is clearly evidenced from the first deintercalation step studied ($x = 0.15$) by the appearance of another sub-spectrum with an isomer shift in the range −0.17 to −0.01 mm s^{-1} and a quadrupole splitting of 0.38–0.15 mm s^{-1}. These parameters are characteristic of Fe^{IV} and indicate that Fe^{IV} atoms are probably located on tetrahedral sites as previously described from ^{57}Fe Mössbauer measurements on $Li_xNi_{1-y}Fe_yO_2$ [17] or $Li_xCo_{0.8}Fe_{0.2}O_2$ [9]. In addition, for $y = 0.1$, $y = 0.2$ and $x = 0.15$, one can observe that the first Fe^{III} atoms oxidised are those located on the tetrahedral sites. These two results indicate a preference of Fe^{IV} ions for the tetrahedral sites, and support the assumption of a partial ion migration during deintercalation, that has already been discussed in Ref. [6,7]. For $0.15 \leq x \leq 0.60$, the oxidation of Fe^{III} to Fe^{IV} continues with increasing lithium deintercalation. In addition, it should be noted that the quadrupole splitting values (which are in the range 0.38–0.15 mm s^{-1}) are consistent with a decrease of the coordination number (CN) from 6 to 4, in agreement with Fe^{IV} in tetrahedral sites. This is also consistent with a previous EXAFS study [7], which showed that CN(Fe) is

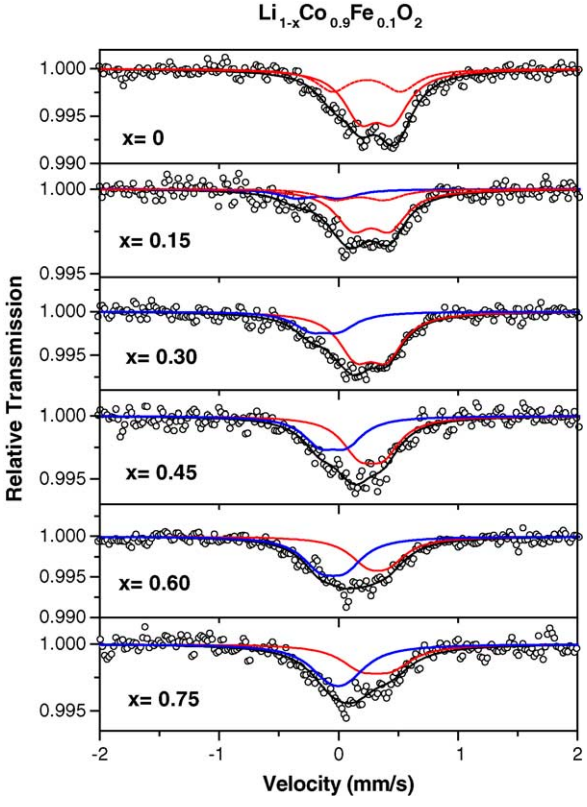

Fig. 3. ^{57}Fe Mössbauer spectra of $Li_{1-x}Co_{0.9}Fe_{0.1}O_2$ recorded on plastic battery during the first charge.

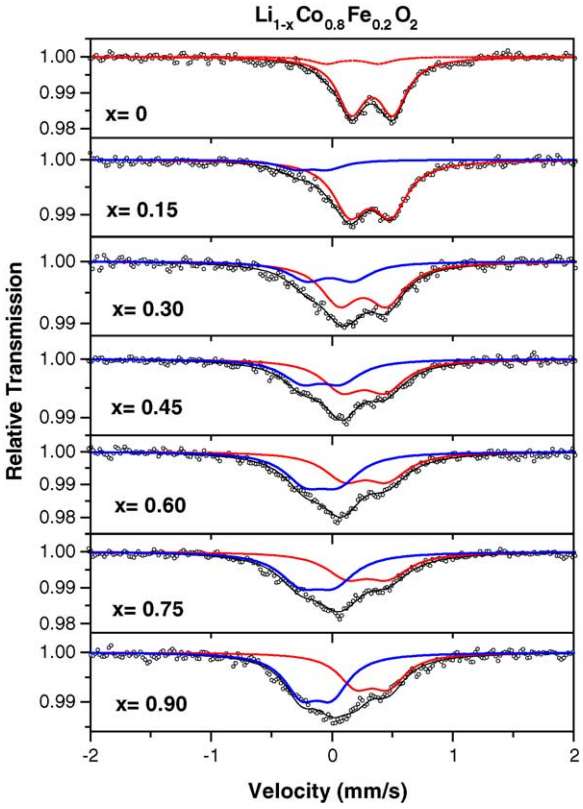

Fig. 4. ^{57}Fe Mössbauer spectra of $Li_{1-x}Co_{0.8}Fe_{0.2}O_2$ recorded on plastic battery during the first charge.

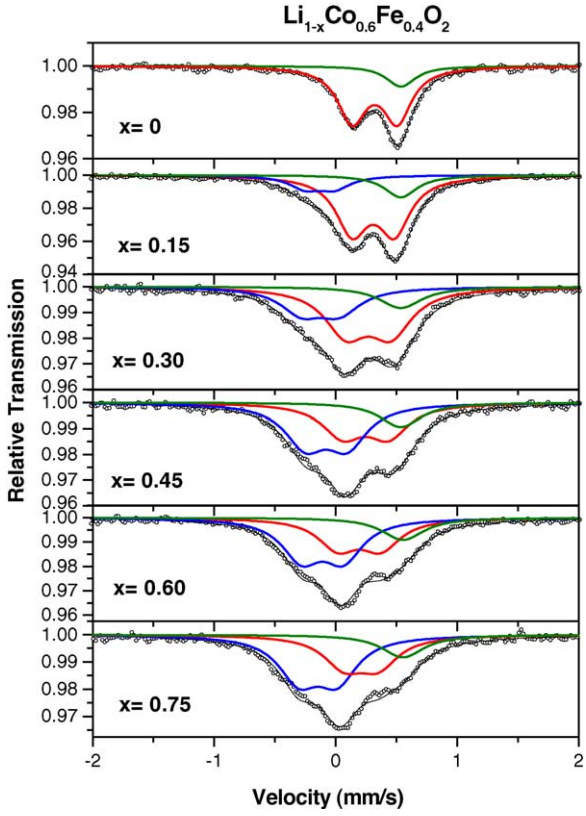

Fig. 5. ^{57}Fe Mössbauer spectra of $Li_{1-x}Co_{0.6}Fe_{0.4}O_2$ recorded on plastic battery during the first charge.

reduced from 6 to 4 in the case of the iron atoms, whereas CN(Co) remains equal to 6 during the delithiation process. As shown in Fig. 6 and for $x \leq 0.60$, the amount of oxidised iron is directly proportional to the number of deintercalated lithium atoms.

For $x > 0.60$ the relative contribution of the Fe^{IV} sub-spectrum remains approximately constant, which indicates that iron is no longer involved in the oxidation process, but that only Co^{III} ions are oxidised further.

The results show that the oxidation of iron is possible and confirm the combined X-ray diffraction and absorption analysis [6,7]. However, the oxidation of Fe^{III} occurs simultaneously with that of Co^{III} only until half the iron is oxidised to Fe^{IV}. At this stage the matrix effect of Co^{III} [7] seems to operate well for all three compositions. This is somewhat in contrast with the results of our previous XANES study, where it was concluded that only in cobalt-rich samples ($y = 0.1$ and 0.2) the oxidation of Co^{III} and Fe^{III} occurs simultaneously, whereas in the iron-rich sample ($y = 0.4$) the Co^{III} ions are oxidised first [7]. However, in the XANES study, a structural effect had been found to interfere in the edge energy shift with increasing mean oxidation state of the transition metal ions, which made the edge energies diminish again for the lowest lithium contents in the case of the $y = 0.1$ and 0.2 samples. This was attributed to the appearance of a new phase, which does not form for $y = 0.4$. It may, hence, be possible that the different amount of Fe^{III} present in tetrahedral sites in the pristine samples and different structural behaviour in the $y = 0.4$ sample cause a different behaviour in the XANES study during the delithiation of the sample. Mössbauer spectroscopy provides a direct determination of the iron oxidation state, without interference of such other effects, so that it can be concluded that the oxidation of Fe^{III} to Fe^{IV} occurs simultaneously with the oxidation of Co^{III} to Co^{IV} for all three samples. The oxidation of Fe^{III}, however, does not exceed about half the total amount of iron. This proves that the difficulty of stabilising large amounts of Fe^{IV} in these layered

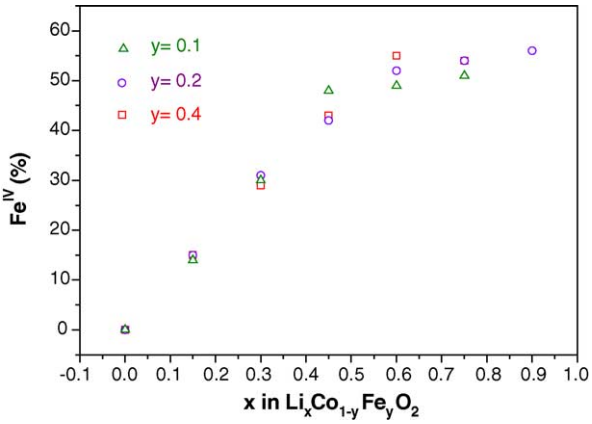

Fig. 6. Relative contribution of the Fe^{IV} sub-spectrum to the total absorption as a function of the amount of deintercalated lithium.

oxides, together with the migration of the Fe^{IV} to tetrahedral sites, is the reason why iron-containing layered oxides with the α-$NaFeO_2$-structure do not deintercalate lithium with a high reversibility.

Acknowledgment

The authors thank M. Morcrette (LRCS, University of Amiens, France) for his contribution in plastic battery assembly.

References

[1] T. Tanaka, K. Ohta, N. Arai, J. Power Sources 97–98 (2001) 2.
[2] I. Saadoune, M. Ménétrier, C. Delmas, J. Mater. Chem. 7 (1997) 2505.
[3] M. Holzapfel, C. Haak, A. Ott, J. Solid State Chem. 156 (2001) 470.
[4] R. Alcántara, J.C. Jumas, P. Lavela, J. Olivier-Fourcade, C. Pérez-Vicente, J.L. Tirado, J. Power Sources 81–82 (1999) 547.
[5] M. Holzapfel, R. Schreiner, A. Ott, Electrochim. Acta 46 (2001) 1063.
[6] M. Holzapfel, P. Strobel, C. Darie, J. Wright, M. Morcrette, E. Chappel, M. Anne, J. Mater. Chem. 14 (2004) 94.
[7] M. Holzapfel, O. Proux, P. Strobel, C. Darie, M. Borowski, M. Morcrette, J. Mater. Chem. 14 (2004) 102.
[8] H. Kobayashi, H. Shigemura, M. Tabuchi, H. Sakebe, K. Ado, H. Kageyama, A. Hirano, R. Kanno, M. Wakita, S. Morimoto, S. Nasu, J. Electrochem. Soc. 147 (2000) 960.
[9] V. McLaren, A.R. West, M. Tabuchi, A. Nakashima, H. Takahara, H. Kobayashi, H. Sakaebe, H. Kageyama, A. Hirano, Y. Takeda, J. Electrochem. Soc. 151 (2004) A672.
[10] L. Aldon, P. Kubiak, A. Picard, P.E. Lippens, J. Olivier-Fourcade, J.C. Jumas, Hyperfine Interact. 156/157 (2004) 281.
[11] M. Morcrette, Y. Chabre, G. Vaughan, G. Amatucci, S. Patoux, C. Masquelier, J.M. Tarascon, Electrochim. Acta 47 (2002) 3137.
[12] W. Künding, Nucl. Instrum. Meth. 75 (1969) 336.
[13] J.N. Reimers, E. Rossen, C.D.W. Jones, J.R. Dahn, Solid State Ionics 61 (1993) 335.
[14] F. Menil, J. Phys. Chem. Solids 46 (1985) 763.
[15] M. Georges, A. Fatseas, S. Lefebvre, C.R. Acad. Sci. Paris 266 (1968) 374.
[16] M. Tabuchi, S. Tsutsui, C. Masquelier, R. Kanno, K. Ado, I. Matsubara, S. Nasu, H. Kageyama, J. Solid State Chem. 140 (1998) 159.
[17] J.R. Mueller-Neuhaus, R.A. Dunlap, J.R. Dahn, J. Electrochem. Soc. 147 (2000) 3598.